WATER IMPACT LOADS ON PRISMATIC BODIES

Melvin E. Hathaway

National Advisory Committee for Aeronautics

Introduction

The overall objective of NACA hydrodynamic research, which must be kept in mind during all stages of our work, is to obtain and present information which will be of use to a designer in building an adequate or better vehicle for operation on water. In these days especially, the vehicle may be of almost any shape from that required for seaplane hulls, to floats for a helicopter, or even the nose cone of a space rocket. The vehicle may have almost any weight or loading from tons per square foot on a hydro-ski or nose cone, to a few pounds per square foot on a helicopter float. The body may strike the water in free fall or it may be largely supported by wings or parachute. It may strike vertically or tangentially, and the water surface is practically never smooth but of varying roughness. To make things really complicated, the body is not rigid but is usually an extremely complex elastic structure having many modes of vibration. Some modes of large amplitude will affect the behavior and applied loads, and others will affect only the stresses and fatigue life of the structure. To investigate all these problems in detail is impractical. To a considerable extent the work consists of testing quite rigid, dynamically similar models of rather specific characteristics and under greatly simplified conditions. These tests can only yield approximations as to behavior and loads of the full-scale vehicle under actual operating conditions. Flight tests are therefore required as a final step in verifying the results. Although most of the research is experimental, considerable effort has been devoted to analytical investigations of certain simplified cases of shape, structure, and conditions, since advances in generalization and prediction result in tremendous savings in test effort.

The theoretical work on water impact loads has been substantially limited to consideration of loads on rigid prismatic bodies having straight-sided V-bottoms, and the data to be presented are for fixed-trim impacts in smooth water. Expressions for the generalized variables are given but equations of motion, derivations, and detailed discussions of theory will be found in the references. A complete list of symbols is given at the end of the paper.

Figure 1 shows the important variables and illustrates the treatment of impacts on waves. We assume a rigid body whose weight W is at all times balanced by a force L applied by a wing or other lifting device. The body

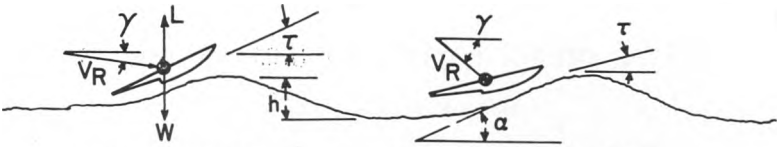

α = WAVE SLOPE AT POINT OF IMPACT

τ = TRIM ANGLE

γ = FLIGHT PATH ANGLE

W = LANDING WEIGHT

V_R = RESULTANT VELOCITY

V_N = VELOCITY NORMAL TO KEEL

$\tau - \alpha$ = EFFECTIVE TRIM ANGLE

$\gamma + \alpha$ = EFFECTIVE FLIGHT PATH

L = WING LIFT

V_V = VELOCITY NORMAL TO WATER SURFACE

V_P = VELOCITY PARALLEL TO KEEL

FIG. 1. DEFINITION SKETCH.

is at a trim angle τ and has a velocity V_R which is at an angle γ to the horizontal. Contact with the water is made at a point on a wave where the local water surface has a slope α. The wave whose surface has the slope α is assumed to be sufficiently large to permit the full length of the model to be immersed in an approximately planar surface and each contact with the water is considered to be an isolated impact having its own initial conditions which are either assumed or obtained from dynamic model tests. The loads developed by this impact on a wave are considered to be the same as those for a smooth water impact having the same attitude and velocity components taken with respect to the water surface. In some cases, an additional refinement consists in combining the orbital velocity of the water at the point of contact with the velocity components of the body. The treatment of rough water is thus reduced to considering only smooth water impacts having an effective trim angle $\tau - \alpha$ and an effective flight path angle $\gamma + \alpha$ with all initial conditions arbitrarily determined from dynamic model results or full-scale operational data.

The geometry of a smooth water impact is shown in Fig. 2, where a portion of a flying-boat hull is indicated. For some distance forward from the step, the bottom is assumed to be a flat-sided wedge having an angle of dead rise β with the axis or keel inclined to the water surface at an angle τ. This wedge makes contact with the water at a velocity V_R inclined to the water surface at an angle γ. The velocity components in space are V_H the horizontal and V_V the vertical. With respect to the keel of the body, the resultant

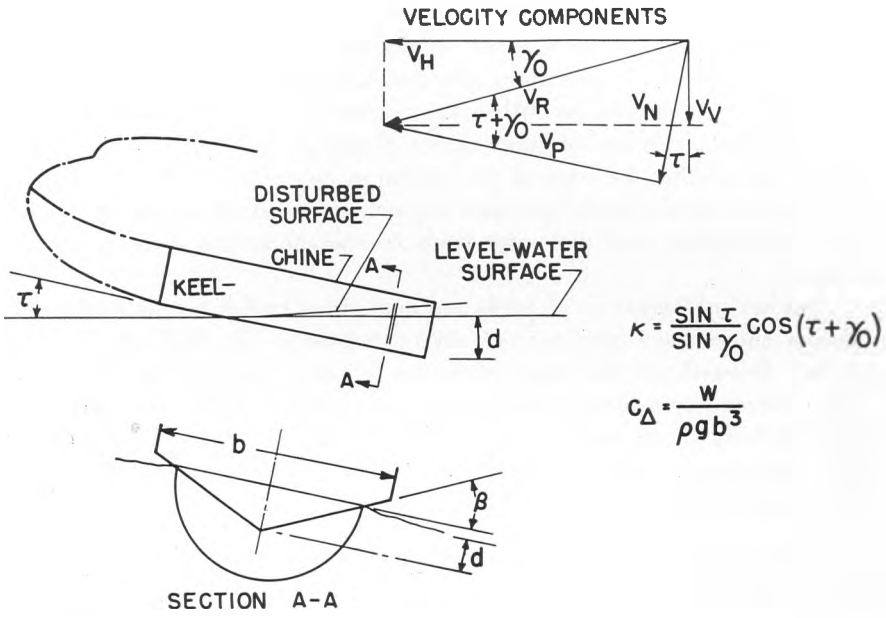

FIG. 2. GEOMETRY OF IMPACT.

velocity has a component normal to the keel V_N and along the keel V_P. The definitions of approach parameter κ and Froude load coefficient C_Δ should be noted since they will be needed to interpret the following figures.

The early impact theory of Kármán [1] was based on the principle of conservation of momentum throughout the impact. Prior to impact all momentum is associated with the body, but as the wedge becomes immersed part of the momentum is imparted to a mass of water which is in contact with the bottom and which has the same velocity as the bottom. With a constant momentum, increased mass required a decreased velocity for the system and the change of momentum of the body alone defined the force on the body. Kármán proposed an attached or virtual mass equal to the mass of a half-cylinder of water having a diameter equal to the instantaneous width of the wedge in the plane of the undisturbed water surface.

Wagner [2,3] obtained improved values for the virtual mass by taking into account the rise of the water surface near the wedge. Pabst [4] and others made contributions which improved the agreement between theory and experiment, if the resultant velocity was normal to the keel.

It was pointed out by Mayo [5] of the NACA Impact Basin that velocity along the keel resulted in virtual mass and momentum being shed from the step and left behind in the wake. His equations, still based on momentum considerations, included the effect of velocity along the keel and are valid

for the entire range of oblique impact.

Derivation of a factor κ which relates the combined effect of velocity components normal to and along the keel, together with a generalization of the equations, was given by Milwitzky in a report [6] which also takes into consideration the effects of finite chines. When the water surface, including water rise, reaches the edge of the bottom at any section, the virtual mass for that section no longer increases but remains constant during any subsequent penetration and the water loads on the submerged sections are decreased.

Further investigations of loads and motions of bodies having deeply immersed chines have been carried out by Schnitzer [7], Shuford [8], and others. Research on this class of bodies is being pursued because of the large reductions in loads which can be achieved by limiting the size of the body striking rough water at high speed. It should be mentioned that, for the same reason, research on hydrofoils also is being vigorously pursued by Wadlin and others [9] at the NACA and elsewhere.

ANALYTICAL AND EXPERIMENTAL RESULTS

Impact Without Chine Immersion

The next eight figures are based on illustrations from Milwitzky's report in which he derives the results and presents them in more detail than can be done here. The basic assumptions to be remembered are that the body is a rigid wedge of sufficient width that the chines do not become immersed, has a fixed angle of dead rise and a finite trim angle which remains constant throughout the impact. It is further assumed that gravitational and viscous forces are negligibly small in comparison with the inertial forces.

The relationship, in a generalized form, of the variation of draft with time during an impact is shown in Fig. 3. The ordinate is the generalized draft which is defined as the product of the instantaneous draft and a function of the initial conditions. The abscissa is generalized time which is defined as the product of time, measured from initial water contact, and a function of the initial conditions. Computed curves are shown for several values of κ; the points are measured experimental values multiplied by the appropriate function of the initial conditions. These experimental data were obtained at the NACA Impact Basin from large models which were tested at weights of 1000 to 2500 pounds. The range of test conditions was greater than can be obtained in flight tests since they were not limited by considerations of pilot safety. Specialized equipment and instrumentation were used to control the conditions and to measure the transient loads and motions with considerably greater accuracy than can be obtained during flight tests. Comparisons of flight-test and Impact Basin data for the same test conditions have shown very good agreement. The agreement between theory and Impact

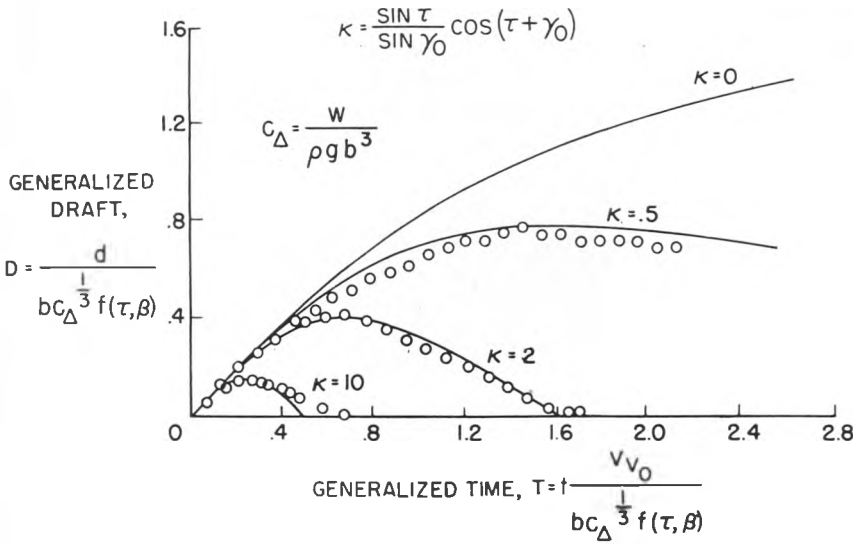

FIG. 3. DRAFT VARIATION WITH TIME—WITHOUT CHINE IMMERSION.

Basin data shown here is good for all practical purposes. Detailed study indicates that the major discrepancies shown are due to fundamental shortcomings in equipment and instrumentation, such as mechanical friction and time lags in the instruments.

A number of observations can be made from the definitions of the generalized variables shown on this figure. One can see that for each value of κ there is a single displacement curve but that any value of κ can be obtained from various combinations of trim angle τ and flight-path angle γ.

Inspection of the definition for draft shows that for a given body geometry and κ, i.e., for fixed values of dead rise, trim and flight-path angle, the draft d is independent of speed and varies directly as the cube root of the loading or mass of the model $bC_\Delta^{1/3}$. To be noted is the fact that C_Δ contains b^3 in the denominator so that b disappears from $bC_\Delta^{1/3}$ and for prisms without chine immersion the draft is completely independent of the geometric beam. In other words, the draft and wetted beam depend solely on the weight and geometry of the body and flight path. For the same fixed geometry the time t to any stage of the impact also varies directly with the cube root of the loading, but it also varies inversely as the vertical velocity.

Changes of draft or time associated with changes in geometry are much more complex, and appropriate values of κ and $f[\tau,\beta]$ must be used. The function of τ and β includes the effect of dead rise and aspect ratio as well as trigonometrical functions of τ.

Discussion and suggested values for this function of τ and β are contained in several of the references and for these data specifically in Milwitzky's report. The function is left in a general form for the purpose of using improved values as they are derived or obtained experimentally.

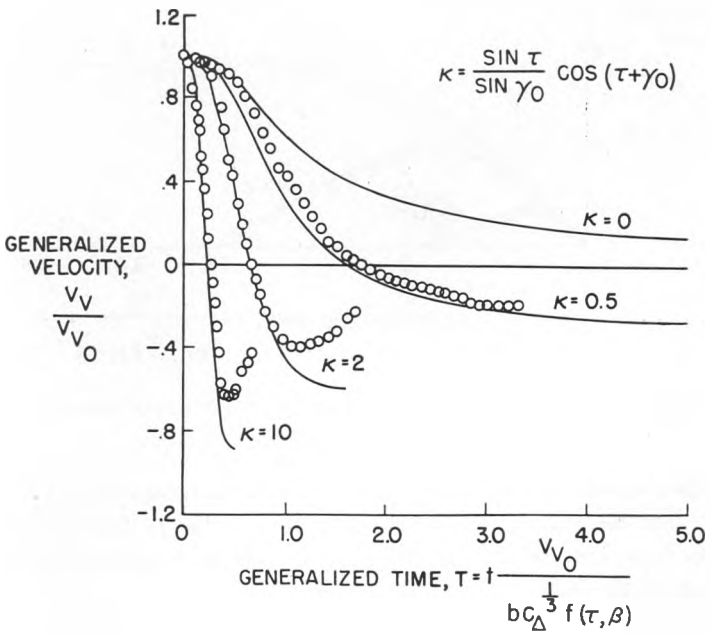

FIG. 4. VARIATION OF VERTICAL VELOCITY WITH TIME—WITHOUT CHINE IMMERSION.

In Fig. 4 the variation of vertical velocity with time which occurs during an impact is shown. The ordinate is the ratio of vertical velocity, at any instant during the impact, to the initial vertical velocity. The abscissa, as in the previous figure, is the generalized time T. The lines have been computed for several values of κ and the points are measured values obtained experimentally at the corresponding values of κ. The agreement between theory and experiment is good during most of the impact but the measured upward velocity at and near exit is considerably less than the computed velocity. These differences are known to be largely due to unavoidable inertia, friction, and pressure losses in the apparatus used in the experiments at the Impact Basin to simulate wing lift.

The variation of acceleration with time for several sets of initial conditions κ is shown in Fig. 5. The abscissa is again generalized time and the ordinate is generalized acceleration. Curves are shown for several values of κ and the points are measured values for κ of approximately 0.5, 2, and 10.

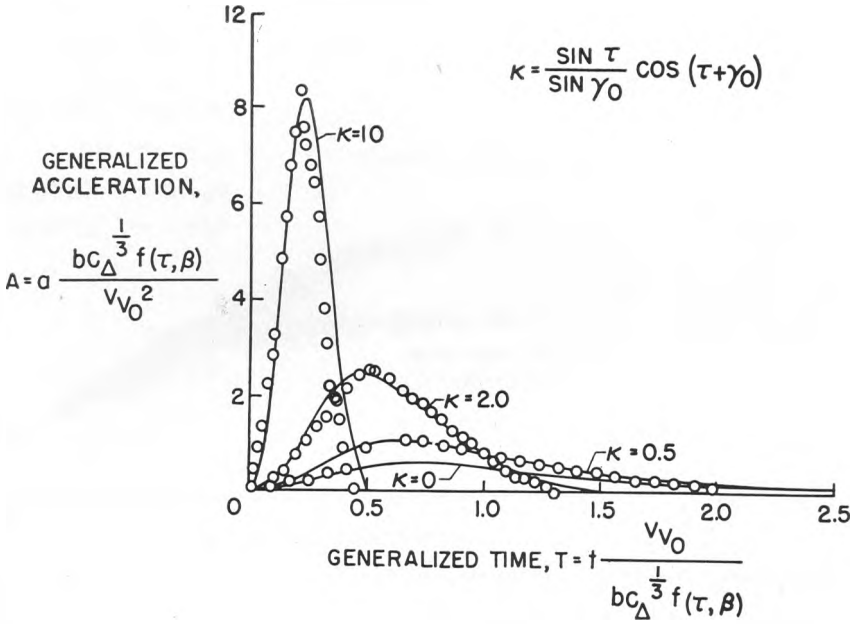

FIG. 5. VARIATION OF ACCELERATION WITH TIME—WITHOUT CHINE IMMERSION.

As in the previous figure and for the same reasons, the largest difference between computed and experimental values is found in the latter stages of the impact near exit. From the expression for generalized acceleration, it can be seen that, for a given body geometry ($f[\tau,\beta]$ = constant) and set of initial flight conditions (κ = constant), the acceleration varies directly with the square of the initial vertical velocity ($V_{V_0}^2$). As in the case of the draft, b disappears from the expression $bC_\Delta^{1/3}$ so that the acceleration is also completely independent of the beam and varies inversely as the cube root of the weight.

Since all the generalized variables are based on the initial downward velocity, all the generalized curves may be interpreted as corresponding to dimensional curves for impacts with the same downward velocity but different flight path angles and, therefore, different forward speeds. In this case the effect of κ on the dimensional variables is the same as on the generalized variables.

On the other hand, if the resultant velocity were to be considered constant and the flight path or downward velocity were allowed to vary, the dimensional curves for different values of κ would not have the same relative shapes as the generalized curves.

Figure 6 shows the variation with κ of draft at maximum acceleration and

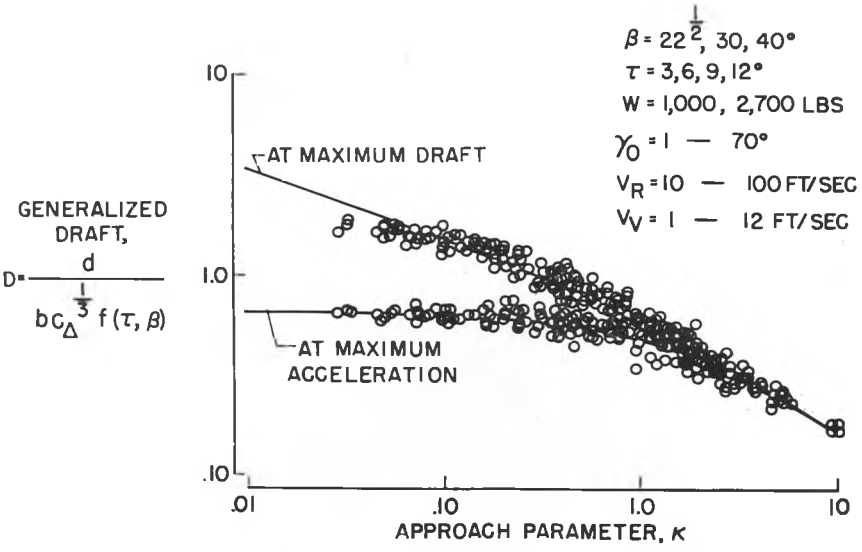

FIG. 6. DRAFT VARIATION WITH APPROACH PARAMETER—WITHOUT CHINE IMMERSION.

at maximum draft. The ordinate is the generalized draft as in Fig. 3 but the abscissa is the approach parameter κ. The curves have been computed from theory and the points again have been obtained from measurements made during tests of several prismatic bodies. All the data obtained during several years of testing are here shown condensed to single curves. The test data cover a considerable range of shapes, weights, velocities, and flight-path angles. Logarithmic scales are used in order to spread out the test data and to emphasize the differences in the various stages of the impact. The scatter of the mass of data is about the same as the scatter of data from each test.

This figure shows, as might be reasonably expected, that the greater drafts occur at the higher flight-path angles which are associated with small values of κ. Similarly, the difference between maximum draft and the draft at the instant of maximum acceleration is greatest at low values of κ which correspond to drop tests, decreases as the flight-path angle is reduced, and is quite small for most flight-test data.

The expression for generalized draft indicates that for any given value of κ the absolute draft, at any stage of the impact, is independent of the magnitude of the initial velocity and the size of the prism. This fact is borne out by the test data, which include an 8 to 1 velocity range. This figure also indicates that the maximum draft at low values of κ tends to be slightly less than that specified by theory. This might be expected since the theory neglects the lift due to buoyancy, which becomes appreciable at deep drafts.

Generalized vertical velocities at the instants of maximum acceleration

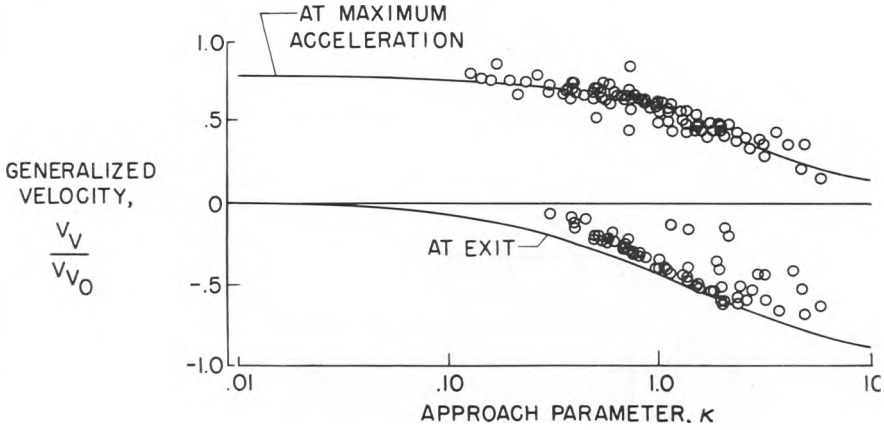

FIG. 7. VARIATION OF VELOCITY RATIO WITH APPROACH PARAMETER—WITHOUT CHINE IMMERSION.

and exit are indicated in Fig. 7. The ordinate is the ratio of vertical velocity at a given instant to the initial vertical velocity and the abscissa is again the approach parameter κ. The experimental points scatter about the theoretical curves and at low κ measured velocities at exit have been omitted as not applicable, since after maximum acceleration the chines or edges of the prisms become immersed, thus violating the requirement of fixed geometry. The scatter evident in the test data is largely due to the errors inherent in

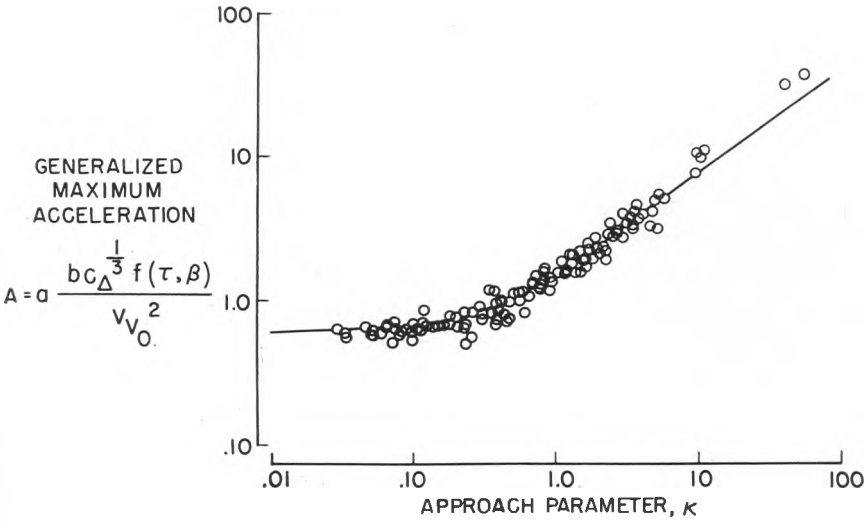

FIG. 8. VARIATION OF MAXIMUM ACCELERATION WITH APPROACH PARAMETER—WITHOUT CHINE IMMERSION.

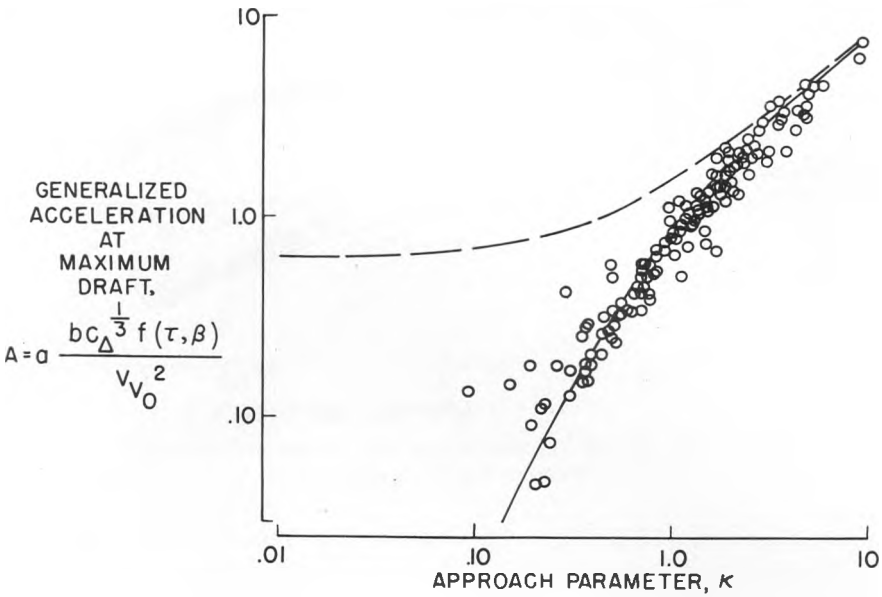

FIG. 9. ACCELERATION AT MAXIMUM DRAFT AS A FUNCTION OF APPROACH PARAMETER—WITHOUT CHINE IMMERSION.

correlating independent measurements from instruments having small but appreciable time lags.

The variation of maximum acceleration with the approach parameter κ is shown in Fig. 8 in which the ordinate is the generalized acceleration. The scatter of the experimental points about the theoretical line indicates reasonable agreement for the entire range of parameters investigated. Improvement in instrumentation during these tests resulted in substantially less scatter of the latest data points, which are not specifically identified on this figure. Some of the data spread below the curve may also be due to load reductions resulting from a small amount of chine immersion.

The same theoretical curve of maximum acceleration is shown as a dashed line in Fig. 9; the solid line is the theoretical variation of acceleration at maximum draft d with the approach parameter κ. It should be mentioned again that a considerable amount of data at small values of κ have been omitted because of the large chine immersion which occurred after maximum acceleration but prior to maximum draft. A substantial amount of chine immersion reduces the maximum acceleration but increases the acceleration at maximum draft so that data having various amounts of chine immersion would tend to fill in the area between the curves shown here.

Figure 10 shows the variation of time T with approach parameter κ for

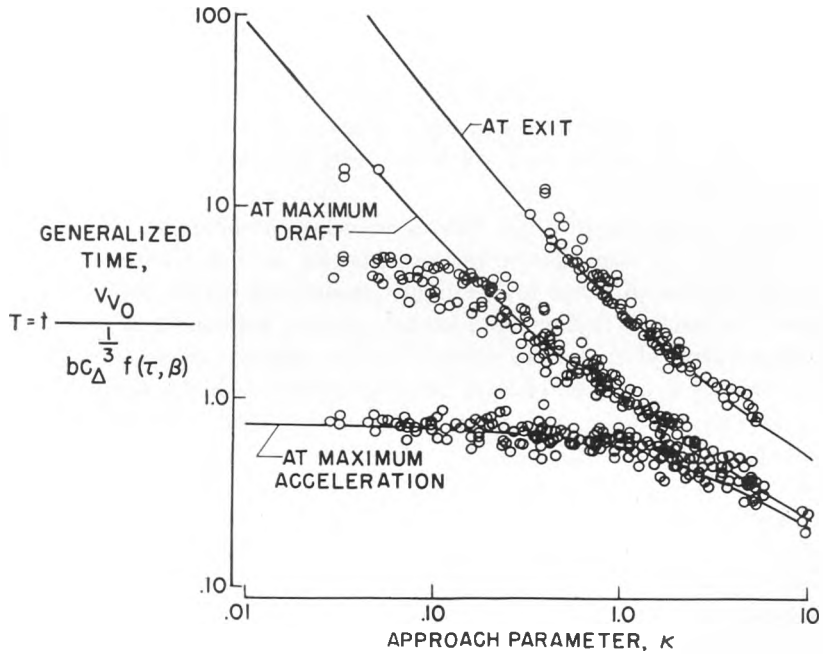

FIG. 10. TIME VARIATION WITH APPROACH PARAMETER—WITHOUT CHINE IMMERSION.

the instant of maximum acceleration, maximum draft, and exit. The ordinate is generalized time, which is defined as the absolute or elapsed time from the instant of contact, multiplied by a function of the initial conditions for the impact. The experimental data are in substantial agreement with theory and much of the scatter can be attributed to errors in picking the instant at which each event occurred. Even a slight amount of structural oscillation can distort a record and make time determinations inaccurate, especially if the record peak is broad or flat.

It may be of interest that at zero value of κ, because of the omission of buoyancy, the theory predicts that maximum draft would never be reached and the data on this figure show steadily increasing time to reach maximum draft as κ becomes small. This figure also shows the small difference in time between maximum acceleration and acceleration at maximum draft for the large values of κ which occur as the planing condition is approached.

The data presented up to this point have been for lightly loaded prisms which do not have the chines or edges immersed in the water at any stage of the impact. For this condition the magnitude of the loads and motions increases rapidly as the severity of the approach conditions, speed and flight path, increases. Chine immersion prior to maximum load can substantially decrease the loads and is, therefore, of practical interest to designers.

Impact with Chine Immersion

The next figures are similar to those which have been shown but are for heavily loaded prisms which have their chines immersed early in the impact before maximum load is reached. These figures are based on a report by Schnitzer [7] and on data which are being prepared for publication by Markey of the NACA.

Before examining the next figures in detail it should be pointed out that, although the same generalized variables are used, the functions of trim and dead rise are different for the lightly loaded and for the heavily loaded prisms. For instance, in the lightly loaded case, i.e., without chine immersion, the aspect ratio of the wetted surface remains constant throughout the impact under the assumption of fixed trim and dead rise. In the heavily loaded case, however, the aspect ratio varies continuously with draft but the function of aspect ratio approaches unity at moderate drafts and remains there for deeper immersions. The expression for κ is the same but the effect of κ on loads and motions is somewhat different for the two cases. The effect of loading is also different in the two cases. The expression for the effect of loading is $bC_\Delta^{1/3}$ for the non-immersed case and $bC_\Delta^{1/2}$ for the deeply immersed case.

In connection with Fig. 3, impact without chine immersion, attention was called to b^3 in the denominator of the expression for C_Δ and it was shown from $bC_\Delta^{1/3}$ that the absolute acceleration was independent of the beam and varied inversely with the cube root of the weight. In the chine-immersed case $bC_\Delta^{1/2}$ reduces to $(W/b)^{1/2}$ which shows that absolute acceleration varies directly with the square root of the geometric beam and inversely with the square root of the weight. Large reductions in acceleration can be

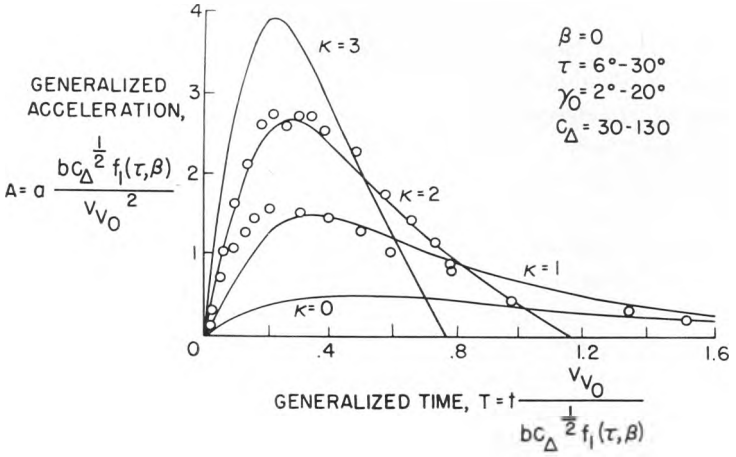

FIG. 11. ACCELERATION VARIATION WITH TIME—IMMERSED CHINES.

obtained by reducing the beam as well as by increasing the loading or sharpening the dead rise.

In Fig. 11 the variation with time of the acceleration of a chine-immersed body having a flat bottom $\beta = 0$ is shown. The ordinate is the generalized acceleration and the abscissa is generalized time. Different geometries are provided for in the function of trim and dead rise $f_1(\tau,\beta)$ for chine-immersed bodies. Theoretical curves are shown for four values of κ ; those for $\kappa = 0$ and $\kappa = 3$ are considered to be approximately the limit of applicability for the chine-immersed impacts. The range between them, however, is quite large and includes most of the severe impacts. The experimental points for $\kappa = 1$ and $\kappa = 2$ are for single impacts but are typical for all the test results.

These points do not show quite as good agreement with theory as did those for the non-chine-immersed case shown in Fig. 5. There is some tendency for theory to give low values for the acceleration early in the impact and high ones late in the impact.

The variation with approach conditions of the draft at the instant of maximum acceleration is plotted on logarithmic scales in Fig. 12 for reasons previously mentioned. The ordinate is the generalized draft at the instant of maximum acceleration. The curve has been computed from theory and the points are from tests of a flat-bottom model. The rather wide scatter of the data is due to inaccuracies in time correlation of the draft and acceleration records, but the theoretical curve is definitely high, especially for values of κ above 3.

Figure 13 shows the variations of maximum draft with κ for chine-immersed prisms. The solid line computed from theory shows somewhat

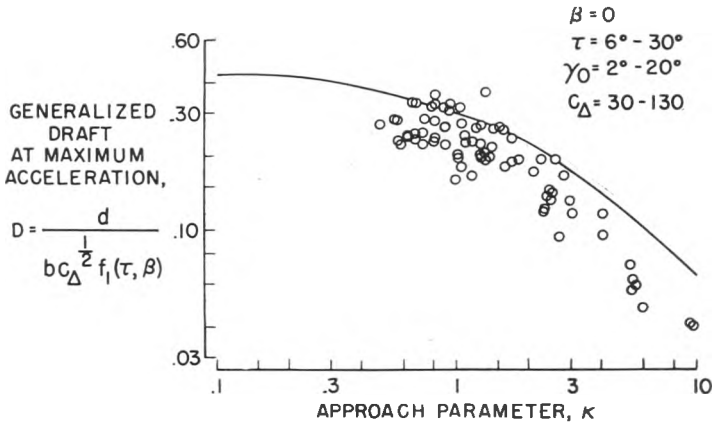

FIG. 12. VARIATION OF DRAFT AT MAXIMUM ACCELERATION WITH APPROACH PARAMETER—IMMERSED CHINES.

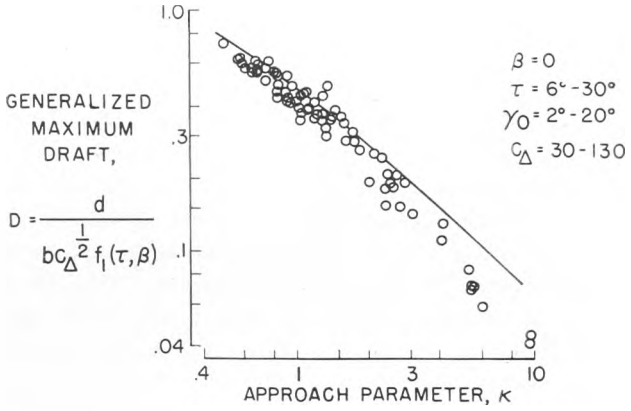

FIG. 13. MAXIMUM-DRAFT VARIATION WITH APPROACH PARAMETER—IMMERSED CHINES.

greater drafts than are found experimentally, particularly for values of κ above 3. The scatter of the experimental points is much less than that seen in Fig. 12 since the measurement of maximum draft did not involve the time correlation required for determining the draft at the instant of maximum acceleration.

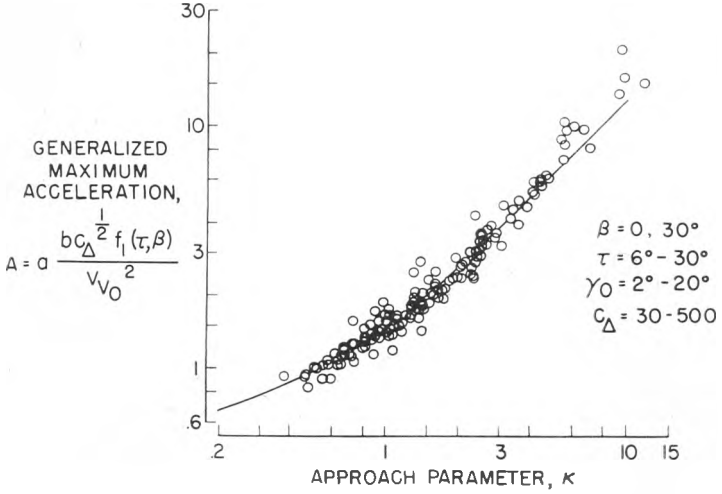

FIG. 14. VARIATION OF MAXIMUM ACCELERATION WITH APPROACH PARAMETER—IMMERSED CHINES.

Figure 14, which shows the variation of maximum acceleration with κ, contains experimental data for both a flat bottom ($\beta = 0°$) and a 30° dead-rise bottom. For values of the beam-loading coefficient C_Δ up to 500, there appears to be reasonably good agreement between theory and

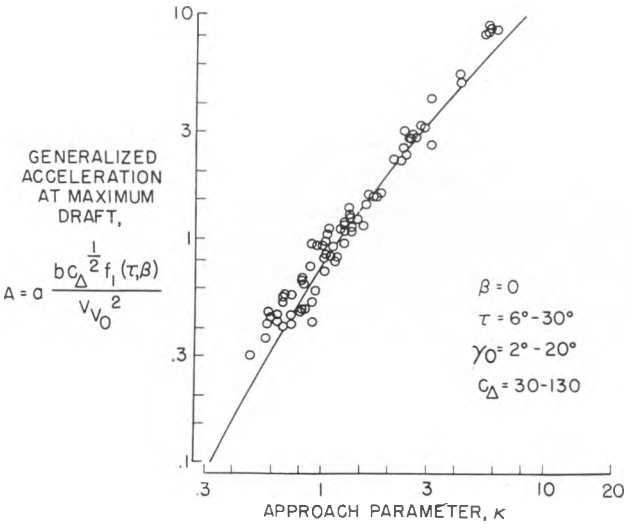

FIG. 15. ACCELERATION AT MAXIMUM DRAFT AS A FUNCTION OF APPROACH PARAMETER—IMMERSED CHINES.

experiment over most of the range of flight conditions defined by κ less than 10.

The variation with κ of acceleration at the instant of maximum draft is shown in Fig. 15; the experimental data are for zero dead rise only. The agreement between theory and experiment is about the same as in Fig. 14.

CONCLUSION

Two separate sets of theoretical and experimental data have been presented for the impact of prisms on a smooth water surface. The first set was for prisms having edges or chines which remain above the water surface throughout the impact. The second set of data was for heavily loaded prisms having a long length of chine immersed before maximum load was reached. There is a rather important gap between these two conditions where only a relatively short length of chine is immersed. For this range of great practical importance individual step by step calculations can be made but satisfactory generalized results have not yet been obtained. Increases in the landing speed of water-based aircraft, together with increased need for operation in rough water or on the open sea, have emphasized the need for research on bodies or lifting surfaces of limited length as well as of limited width. These lifting surfaces, either hydro-skis or hydrofoils, must develop a definitely limited load during and after full immersion of the surface while driving through waves, and they must dissipate vertical

momentum by maintaining an upward force at all depths of immersion. Stable configurations for such devices are being established and both theoretical and experimental research is being continued by the NACA and other investigators.

In conclusion, it may be appropriate to re-state that the oblique impact of prismatic bodies is considered to fall into four classes: nonimmersed chines, partly immersed chines, immersed chines, and fully immersed chines and bow. Data from impacts of prismatic bodies having immersed and nonimmersed chines have been generalized and reasonable agreement between theory and experiment has been demonstrated for a large range of impact conditions. Some observations of practical significance can be made from Fig. 16 which is based on experimentally-verified theoretical

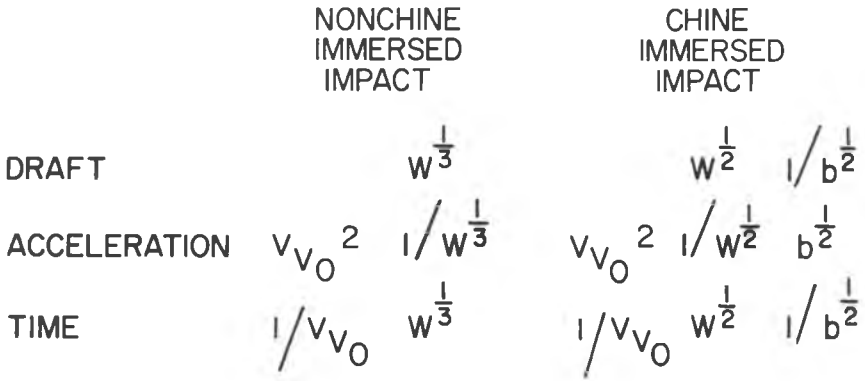

FIG. 16. EFFECT OF DIMENSIONAL VARIABLES ON DRAFT, ACCELERATION, AND TIME.

research. This figure shows, for fixed geometry of body and flight, the dimensional variables which determine draft, acceleration, and time to corresponding points of impact. It can be seen that for both types of impact the draft is independent of velocity, the acceleration varies as the square of the velocity, and time is inversely proportional to velocity. The effect of weight is, however, different for the two types of impact. In one case weight enters to the $\frac{1}{3}$ power and in the other case to the $\frac{1}{2}$ power. It can also be seen that for nonimmersed chines, the size of the body has no effect but that for immersed chines the size of the prism enters to the $\frac{1}{2}$ power. It is this effect of width on acceleration which makes the chine immersed body of interest to designers for reducing water impact loads.

SYMBOLS AND DEFINITIONS

A generalized acceleration $= a\dfrac{bC_{\Delta}{}^{1/3}\, f(\tau,\beta)}{V_{V_0}{}^2}$ nonimmersed chines

$= a\dfrac{bC_{\Delta}{}^{1/2}\, f_1(\tau,\beta)}{V_{V_0}{}^2}$ immersed chines

a absolute or measured acceleration, ft/sec^2

b beam or width of prism, ft

C_Δ Froude load coefficient at rest, $W/\rho g b^3$

D generalized draft $= \dfrac{d}{bC_\Delta^{1/3} f(\tau,\beta)}$ nonimmersed chines

$= \dfrac{d}{bC_\Delta^{1/2} f_1(\tau,\beta)}$ immersed chines

d absolute or measured draft, ft

$f(\tau,\beta)$ function of (τ,β) for nonimmersed chines

$f_1(\tau,\beta)$ function of (τ,β) for immersed chines

g acceleration of gravity, ft/sec^2

h height of wave, ft

L lift force applied to prism, lbs

T generalized time $= t \dfrac{V_{V0}}{bC_\Delta^{1/3} f(\tau,\beta)}$ nonimmersed chines

$= t \dfrac{V_{V0}}{bC_\Delta^{1/2} f_1(\tau,\beta)}$ immersed chines

t time after initial contact with water surface, sec

V velocity, ft/sec

W weight of prism, lbs

α slope of wave at area of impact

β angle of dead rise of prism

γ flight path angle

κ approach parameter $= \dfrac{\sin \tau}{\sin \gamma_0} \cos(\tau + \gamma_0)$

τ trim angle

ρ mass density of water

Subscripts

H horizontal

Max maximum

N normal to keel

P parallel to keel

R resultant

V vertical

0 at instant of initial contact

REFERENCES

1. Kármán, T. von, "The Impact of Seaplane Floats During Landing," *NACA TN 321*, 1929.

2. Wagner, H., "Ueber Stoss- und Gleitvorgänge an der Oberfläche von Flüssigkeiten," *Zeitschrift für angewandte Mathematik und Mechanik*, Vol. 12, August 1932.

3. Wagner, H., "Landing of Seaplanes," *NACA TM 622*, 1931.

4. Pabst, W., "Theory of the Landing Impact of Seaplanes," *NACA TM 580*, 1939.

5. Mayo, W. L., "Analysis and Modification of Theory for Impact of Seaplanes on Water," *NACA Report 810*, 1945.

6. Milwitzky, B., "Generalized Theory for Seaplanes Impact," *NACA Report 1103*, 1952.

7. Schnitzer, E., "Theory and Procedure for Determining Loads and Motions in Chine-Immersed Hydrodynamic Impacts of Prismatic Bodies," *NACA Report 1152*, 1953.

8. Shuford, C. L., Jr., "A Theoretical and Experimental Study of Planing Surfaces Including Effects of Cross Section and Plan Form," *NACA TN 3939*, 1957.

9. Wadlin, K. L., Shuford, C. L., Jr., and McGehee, J. R., "A Theoretical and Experimental Investigation of the Lift and Drag Characteristics of Hydrofoils at Subcritical and Supercritical Speeds," *NACA Report 1232*, 1955.

DISCUSSION

Wallis Hamilton inquired if all of the calculations were based on an arbitrary amount of water being accelerated with the wedge. The speaker explained that until the velocity component along the keel was introduced all of the water was considered to be acting with the bottom. The amount of water acting with the bottom was obtained theoretically from potential flow theory, and the energy in that water represents that required in setting up the flow to infinity. In other words, it is a virtual mass calculation based on potential flow which gives the amount of water.

Hunter Rouse asked if NACA has made any studies of crash landings, that is, landings of land planes on water. The speaker said there had been such tests made and they are known as ditching tests. Specific models have been tested and information resulting has been incorporated in the instructions for operating these land-based aircraft during ditchings. Very little of the information has been incorporated in the design of planes, but ditchings are so infrequent that one can hardly blame the designers for not wanting to modify the shape of a fuselage to get a better-behaving land plane; so part of the effort of NACA in connection with the ditching of land planes, unaltered, has been to develop and investigate the effect of some auxiliary devices which are called "ditching aids." They are also known as "hydro-flaps" and "hydro-skis." In the case of military aircraft merely deflecting a bomb door, or a very little reinforcing with a bomb door in the right place, or sometimes a surface that can be extended to give some hydrodynamic lift near the bow of the airplane, makes the difference between a mankiller and a successful ditching. Even a successful ditching isn't very nice. The NACA has also done some work in connection with the crashing of land planes primarily from the standpoint of the fire hazard —that is, the sources of ignition and methods of control of incipient fires before they actually develop. They have also investigated to some extent the effect of crashes and the location of the passengers within the airplane during crashes. This is an important part of the impact work being done by the NACA.

Captain Wright asked if any observations had been made of the effect of impact on water where compressibility effects may be involved. The reply was that very little has been done. Actually the compressibility of water enters at speeds approaching that of sound in water and the speed of sound in water is very high. It is only during nearly flat impact of a flat body that speeds in water of that magnitude are reached. The instrumentation for the rest of the work has not been capable of handling that condition. The highest-frequency instruments that could be obtained for the investigation still were not fast enough to investigate either the water or the body. A few feeble attempts were made and, if there were design interest in it, funds probably could be obtained to do a little more.